JACS
JOURNAL OF THE AMERICAN CHEMICAL SOCIETY
Communication
pubs.acs.org/JACS

Stabilization of Ruthenium(II) Polypyridyl Chromophores on Nanoparticle Metal-Oxide Electrodes in Water by Hydrophobic PMMA Overlayers

Kyung-Ryang Wee, M. Kyle Brennaman, Leila Alibabaei, Byron H. Farnum, Benjamin Sherman, Alexander M. Lapides, and Thomas J. Meyer*

Department of Chemistry, University of North Carolina at Chapel Hill, CB 3290, Chapel Hill, North Carolina 27599, United States

Supporting Information

ABSTRACT: We describe a poly(methyl methacrylate) (PMMA) dip-coating procedure, which results in surface stabilization of phosphonate and carboxylate derivatives of Ru(II)-polypyridyl complexes surface-bound to mesoporous nanoparticle TiO_2 and nanoITO films in aqueous solutions. As shown by contact angle and transmission electron microscopy (TEM) measurements, PMMA oligomers conformally coat the metal-oxide nanoparticles changing the mesoporous films from hydrophilic to hydrophobic. The thickness of the PMMA overlayer on TiO_2–Ru(II) can be controlled by changing the wt % of PMMA in the dipcoating solution. There are insignificant perturbations in electrochemical or spectral properties at thicknesses of up to 2.1 nm with the Ru(III/II) couple remaining electrochemically reversible and $E_{1/2}$ values and current densities nearly unaffected. Surface binding by PMMA overlayers results in stable surface binding even at pH 12 with up to a ∼100-fold enhancement in photostability. As shown by transient absorption measurements, the MLCT excited state(s) of phosphonate derivatized $[Ru(bpy)_2((4,4'\text{-}(OH)_2PO)_2bpy)]^{2+}$ undergo efficient injection and back electron transfer with pH independent kinetics characteristic of the local pH in the initial loading solution.

Energy storage with solar energy used to create chemical fuels by artificial photosynthesis is an important research area but one with significant challenges. Hurdles exist to high efficiency energy conversion and storage arising from design, scale-up, and long-term stability of devices and components.[1−7] Use of photoelectrochemical cells for solar energy conversion and storage is a promising approach. This includes dye-sensitized photoelectrosynthesis cells (DSPECs), which integrate high band gap oxide semiconductors with the molecular-level light absorption-catalytic properties of molecular assemblies or clusters. The use of molecular assemblies offers the advantage of exploiting chemical synthesis to make rapid and systematic changes in the active components.[8−11] In a DSPEC photoanode, light absorption by a chromophore (dye)−catalyst assembly initiates electron transfer catalysis by excited state injection with subsequent electron transfer activation of the catalyst for water oxidation.[12−15]

Long-term stability of assemblies on metal-oxide surfaces under the working conditions of a DSPEC, most likely over a broad pH range in water, is an essential element of a working device.[16] The long-term performance of DSPECs depends on both the stability of the active forms of surface-bound assemblies and the stability of the assembly on oxide surfaces. Progress has been made in this area.[17−19] In one approach, atomic layer deposition (ALD) is used to create TiO_2 or Al_2O_3 overlayers following surface binding of chromophores, catalysts, and/or chromophore-catalyst assemblies. Remarkably enhanced interfacial stabilities have been observed even at high pH values in aqueous solutions.[16,20] More recently, reductive electropolymerization of vinyl-functionalized polypyridyl complexes has been exploited to achieve high electrochemical and photochemical stabilities even in basic solutions.[21−23]

We report here an alternate, straightforward approach to overlayer stabilization based on poly(methyl methacrylate) (PMMA) overlayers. It provides a simple alternative that results in surface stabilization without significantly modifying the chemical or physical properties of prebound chromophores. PMMA films have been used as a medium for immobilizing chromophores, including $Ru(bpy)_3^{2+}$ (bpy is 2,2′-bipyridine), in an optically transparent, semirigid matrix convenient for photophysical studies.[24−26]

Here we report the use of thin film overlayers of PMMA to stabilize a Ru(II) polypyridyl complex bound to mesoporous, nanoparticle metal-oxide films over the pH range 1−12 in water. Stabilization is accomplished by adding PMMA to metal-oxide films prederivatized with the surface-bound dye by a dip-coating technique. The thickness of PMMA coatings was varied from 0.8−2.1 nm, as measured by transmission electron microscopy (TEM), controlled by varying the concentration of polymer in precursor stock solutions. With PMMA overlayers, up to ∼100-fold enhancements in photostability have been achieved compared to the surface-bound complex without significant perturbation of optical, electrochemical, or excited state properties.

The PMMA overlayer procedure is illustrated in Figure 1. PMMA coatings were added as an overlayer after surface attachment of $[Ru(bpy)_2((4,4'\text{-}(OH)_2PO)_2bpy)]^{2+}$ (**RuP^{2+}**) or $[Ru(bpy)_2((4,4'\text{-}(COOH)_2bpy)]^{2+}$ (**RuC^{2+}**) as chloride salts to mesoporous metal-oxide films, either TiO_2 or conducting

Received: July 10, 2014
Published: September 8, 2014

   dx.doi.org/10.1021/ja506987a | J. Am. Chem. Soc. 2014, 136, 13514−13517

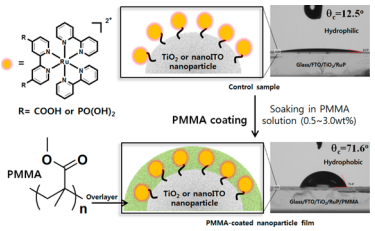

Figure 1. Schematic depictions of an added PMMA coating on a metal-oxide surface (TiO_2 or nanoITO) and the results of contact angle measurements of a mesoporous TiO_2 film before and after soaking in a PMMA/DCM coating solution. Also shown are the chemical structures of the **RuP**$^{2+}$ or **RuC**$^{2+}$ and PMMA ($n \approx 3500$).

Sn(IV)-doped In_2O_3, on fluorine-doped tin oxide (FTO) electrode substrates giving either FTO|TiO_2-**RuP**$^{2+}$ or FTO|nanoITO-**RuP**$^{2+}$. The dipping procedure was performed by brief (seconds) soaking of the derivatized electrodes in dichloromethane (DCM) solutions containing predissolved PMMA oligomer. In order to establish the maximum PMMA wt % in the dipping solutions that still allowed electrochemical activity, cyclic voltammetry was performed on FTO|nanoITO-**RuP**$^{2+}$(PMMA) films following dip-coating in solutions 0.5 wt % to 4.0 wt % PMMA in DCM. As shown in Figure S2, Supporting Information (SI), in 0.1 M $HClO_4$ aqueous solution with up to ~3.0 wt % PMMA, FTO|nanoITO-**RuP**$^{2+}$(PMMA) films retain reversible electrochemistry for the **RuP**$^{3+/2+}$ couple with $E_{1/2}(Ru^{III/II})$ = 1.36 V vs NHE compared to 1.35 V for the surface-bound complex and with a minimal attenuation of current. With 4.0 wt % PMMA in the coating solution, FTO|nanoITO-**RuP**$^{2+}$ films no longer gave an observable electrochemical response for the Ru(III/II) couple presumably due to an inhibition to charge compensation by counterions. Subsequent studies were conducted with ≤3.0 wt % PMMA to avoid electron transfer inhibition.

A similar conclusion was reached from results obtained in a parallel set of experiments on TiO_2 rather than on nanoITO. As shown in Figure S3, SI, **RuP**$^{2+}$ on TiO_2 can be detected electrochemically but with electron transfer inhibited. $E_{1/2}$ for the surface redox couple falls within the semiconductor band gap , and surface oxidation occurs by cross-surface, electron transport to the underlying FTO substrate by site-to-site electron transfer hopping.[27,28]

Contact angle measurements were conducted on PMMA-coated surfaces by using a water droplet method to probe the hydrophobicity of the PMMA coating. As shown in Figures 1 and S4, SI, hydrophobicity of PMMA-coated surfaces is markedly enhanced compared to uncoated surfaces. A linear increase in contact angle was observed with increasing PMMA content in the dip-coating solution with 12.5° (0.0 wt %, control) ≪ 52.6° (0.5 wt %) < 57.1° (1.0 wt %) < 70.7° (2.0 wt %) < 71.6° (3.0 wt %).

Soaking time at fixed concentrations was also investigated as a way to obtain controlled thicknesses. While a minimum soaking time of a few seconds was required, further soaking periods did not lead to significantly thicker coatings. As described above, thickness and morphology of PMMA coatings is dependent on the concentration in the loading solutions.

To provide evidence for conformal PMMA coating throughout oxide films, focused ion beam scanning electron microscopy (FIB-SEM) was used to image PMMA-coated TiO_2-**RuP**$^{2+}$ films. A down cut milling technique was used to expose the inside of the film. As seen in the top view of Figures S5−S9, SI, images of 0.5 wt % to 2.0 wt % PMMA-coated TiO_2-**RuP**$^{2+}$ films show that the

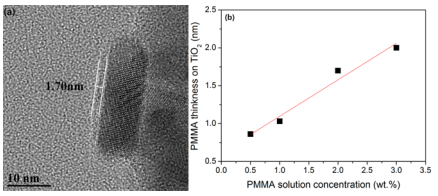

Figure 2. (a) TEM image of a 2.0 wt % PMMA-coated TiO_2 nanoparticle with the PMMA thickness indicated. (b) Variation in PMMA overlayer thickness with solution concentration on TiO_2-**RuP**$^{2+}$.

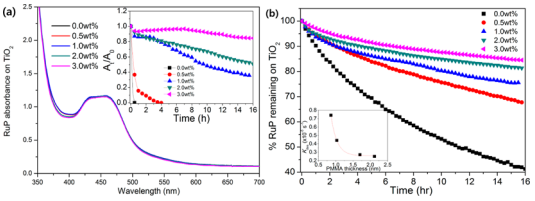

Figure 3. (a) Absorption spectra of TiO_2-**RuP**$^{2+}$ films before and after soaking in 0.5 to 3.0 wt % PMMA solutions. Inset: relative A_t/A_0 absorbances of PMMA-coated TiO_2-**RuP**$^{2+}$ films at 458 nm in pH 12 phosphate buffer solution in the dark. (b) Photostability of a PMMA-coated TiO_2-**RuP**$^{2+}$ film in aqueous 0.1 M $HClO_4$ (pH 1). Inset: desorption rate constant (k_{des}) as a function of PMMA overlayer thickness.

TiO_2 films retain their porosities compared to PMMA-free samples. A molten PMMA layer was observed in cross-sectional images of 1.0 wt % (Figure S7, SI) and 2.0 wt % (Figure S8, SI) PMMA because the organic PMMA overlayer melted under ion beam excitation during the milling process. For 3.0 wt % PMMA, a decrease in porosity was observed along with formation of a thick (~0.4 μm) PMMA layer on top of the mesoporous TiO_2-**RuP**$^{2+}$ film, Figure S9, SI.

These results suggest that overlayers produced from higher concentrations of PMMA (>3.0 wt %) inhibit diffusion of electrolyte solution into the films by blocking the pores of the mesoporous oxide by formation of a thick, nonconformal, blocking layer of PMMA on the outside of the film. The blocked pores inhibit counterion diffusion and impede electrochemical oxidation or reduction.

The PMMA conformal coating thickness on individual TiO_2 nanoparticles was confirmed by transmission electron microscopy (TEM) (Figures S10−S14, SI). Figure 2a shows a TEM image of a 2.0 wt %, 1.70 nm PMMA-coated film on 20−30 nm diameter TiO_2-**RuP**$^{2+}$ nanoparticles. From the TEM images and contact angle data, the PMMA coating appears to form with relative uniformity on individual TiO_2-**RuP**$^{2+}$ nanoparticles with film thicknesses increasing linearly with the wt % of PMMA in the dipping solution, Figure 2b. These results suggest that the adsorbed PMMA overlayers are conformal.

The electrochemical response of **RuP**$^{2+}$ is maintained up to ~2.1 nm (3.0 wt %), a thickness at which the protective overlayer is comparable in thickness to the extended diameters of the surface-bound complexes and associated perchlorate counterions. As shown in Figures 3a and S15, SI, PMMA-coated TiO_2-**RuP**$^{2+}$ and surface-bound nanoITO-**RuP**$^{2+}$ films exhibit the characteristic broad metal-to-ligand charge transfer (MLCT) absorptions from 400 to 550 nm found for other Ru(II) polypyridyl complexes.[29,30] There are additional contributions to the spectra from absorption/scatter on TiO_2, <400 nm, and nanoITO, <350 nm.[27−29] The spectrum of *nano*ITO-**RuP**$^{2+}$ decreases negligibly upon the addition of PMMA overlayers

dx.doi.org/10.1021/ja506987a | J. Am. Chem. Soc. 2014, 136, 13514−13517

showing that it is retained on the surface in the dip coating procedure. In contrast to atomic layer deposited TiO_2 or Al_2O_3 overlayers,[16] only slight spectral shifts are observed in the MLCT absorptions with the shifts due to a PMMA medium effect.[26,31]

Stabilities of PMMA-coated TiO_2-**RuP**$^{2+}$ and nanoITO-**RuP**$^{2+}$ films in aqueous solutions as a function of pH were investigated both in the dark and under irradiation. As shown in Figures S16–S24, SI, the desorption of **RuP**$^{2+}$ from TiO_2-**RuP**$^{2+}$ films, immersed in pure water (pH ≈ 6) and in a pH 12 phosphate buffer solution (0.1 M HPO_4^{2-}/PO_4^{3-} and 0.5 M KNO_3) in the dark were monitored spectrophotometrically over a period of 16 h at 15 min intervals. TiO_2-**RuP**$^{2+}$ is unstable toward surface hydrolysis and desorption of the complex above pH 6 in water (Figures S16 and S20, SI).[17] Desorption was dramatically reduced with added PMMA both in water and in the pH 12 phosphate solution. Stabilization by PMMA was most obvious in the phosphate buffer as shown in the inset of Figure 3a. From these results, more than 90% of the initial **RuP**$^{2+}$ remained after a 16 h soaking period in 3.0 wt % PMMA. Similar stabilizations were observed for nanoITO-**RuP**$^{2+}$ (Figure S38, SI) and TiO_2-**RuC**$^{2+}$ films (Figure S41, SI) under the same conditions in the dark.

Photostabilities as a function of film thickness and pH on both TiO_2 and nanoITO were evaluated by using a previously published protocol with constant irradiation at 455 nm (fwhm ≈ 30 nm, 475 mW/cm^2). **RuP**$^{2+}$ loss from the films was monitored by absorbance changes at 480 nm from 0 to 16 h at intervals of 15 min with corrections made for light scattering. Absorbance changes are shown in Figures S25–S37, SI, for aqueous 0.1 M $HClO_4$, pure water, and the pH 12 buffer solution. For neutral and acidic conditions, desorption kinetics were biphasic with a single average rate constant (k_{des}) calculated as the inverse of the weighted average lifetime ($k_{des} = \langle\tau\rangle^{-1}$). At pH 12 in 0.1 M HPO_4^{2-}/PO_4^{3-} with 0.5 M KNO_3, the kinetics of surface loss were complex but clear evidence for PMMA stabilization was obtained. For films coated from 0.5 wt % PMMA, the surface coverage of **RuP**$^{2+}$ on TiO_2 decreased <∼30% during the 16 h light irradiation period in 0.1 M $HClO_4$, while ∼60% was lost for the control sample. An exponential decrease in k_{des} with overlayer thickness was observed with k_{des} decreased by 20-fold (0.23×10^{-5} s^{-1}) at 3.0 wt % PMMA, Figure 3b.[17]

In a relative sense, photostability was enhanced as the pH was increased. In pure water, k_{des} decreased from $k_{des} > 30 \times 10^{-5}$ s^{-1} without stabilization to 0.31×10^{-5} s^{-1} with 3.0 wt % added PMMA.[16] PMMA overlayers on nanoITO-**RuP**$^{2+}$ displayed similarly enhanced photostabilities (Figures S39–S40, SI) with similar results obtained in acidic and basic solutions.

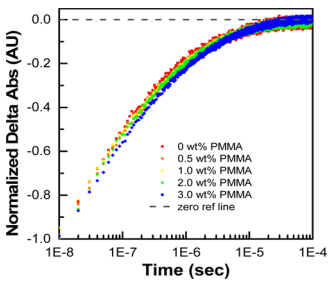

Figure 4. Normalized transient absorbance kinetics probed at 400 nm following 3.2 mJ, 425 nm, 5 ns excitation of TiO_2-**RuP**$^{2+}$(PMMA) electrodes (Γ/Γ_o = 1.0) from ∼3.0 wt % PMMA, immersed in 0.1 M $HClO_4$ at 22 ± 2 °C.

Electronic connection between the oxide surfaces and **RuP**$^{2+}$ through the surface-bound phosphonate groups appears to be maintained through the extended photolysis cycles. As shown by the emission spectra for FTO|TiO_2-**RuP**$^{2+}$ coated from 3.0 wt % PMMA immersed in acid, at pH 7.5 and at pH 12 in Figures S45 and S46, SI, there is no change in the weak emission from the complex even after extended photolysis periods. If the complexes were desorbed from the surfaces and trapped in the PMMA overlayer, an enhancement in emission would have been expected.

The impact of PMMA overlayers on electron injection and recombination kinetics for FTO|TiO_2-**RuP**$^{2+}$ was investigated by nanosecond transient absorption measurements. Figure 4 illustrates back electron transfer recombination kinetics probed at 400 nm, an isosbestic point for the excited state, following 425 nm excitation. The excitation–injection sequence is illustrated in eqs 1–4. Although there are minor differences with and without the PMMA overlayer, the kinetic behavior is similar and essentially independent of the extent of PMMA loading. Quantifying the extent of electron injection was problematic due to the change in the index of refraction from PMMA infiltration, which augments the transient absorption response. Nevertheless, from the data in Figure 4 and the absence of emission, injection is efficient.

$$\text{FTO|TiO}_2\text{-}\mathbf{RuP}^{2+} \xrightarrow{h\nu} \text{FTO|TiO}_2\text{-}\mathbf{RuP}^{2+*} \quad (1)$$

$$\text{FTO|TiO}_2\text{-}\mathbf{RuP}^{2+*} \rightarrow \text{FTO|TiO}_2(e^-)\text{-}\mathbf{RuP}^{3+} \quad (2)$$

$$\text{FTO|TiO}_2(e^-)\text{-}\mathbf{RuP}^{3+} \rightarrow \text{FTO|TiO}_2\text{-}\mathbf{RuP}^{2+} \quad (3)$$

Back electron transfer kinetics for FTO|TiO_2-**RuP**$^{2+}$(PMMA, 3.0 wt %) were monitored at 400 nm as a function of pH and solution composition (Figure S42, SI). Analysis of the data shows that back electron transfer kinetics are independent of pH and relatively independent of the thickness of the PMMA overlayer. The absence of a pH dependence is a striking observation in light of the known pH dependence of recombination kinetics for **RuP**$^{2+}$ and other surface-bound Ru chromophores on nanocrystalline TiO_2.[27,30] In earlier studies on FTO|TiO_2-**RuP**$^{2+}$, back electron transfer was shown to occur by fast and slow components with the slow component (τ >10 μs) representing 15% of the total absorbance change at pH 1, increasing to 30% by pH 5.[27] Our results point to control of the effective surface pH by the PMMA overlayer with surface pH frozen at the pH used in the surface loading solution.

The ability of the PMMA-protected chromophore to undergo sustained electron transfer mediation with an external redox couple was investigated at pH 7 in a 0.1 M phosphate buffer ($H_2PO_4^-/HPO_4^{2-}$) in 0.4 M $NaClO_4$ with hydroquinone (20 mM, H_2Q) added as sacrificial electron transfer donor. In a photoelectrochemical cell with a FTO|TiO_2-**RuP**$^{2+}$ photoanode, Pt cathode, and Thor Laboratories HPLS-30-04 white light source, a sustained photocurrent response was obtained (Figure S47, SI) due to reduction of surface-bound **RuP**$^{3+}$ by H_2Q, eq 4. For a 1.0 wt % PMMA coated film, the photocurrent decreased less than ∼10% during a 900 s irradiation period, while ∼30% was lost for an unprotected control sample due to desorption of **RuP**$^{2+}$.

$$\text{FTO|TiO}_2\text{-}\mathbf{RuP}^{2+} \xrightarrow{h\nu} \text{FTO|TiO}_2(e^-)\text{-}\mathbf{RuP}^{3+} \quad (4)$$

$$\text{FTO|TiO}_2(e^-)\text{-}\mathbf{RuP}^{3+} + 1/2\text{H}_2\text{Q} \rightarrow \text{TiO}_2\text{-}\mathbf{RuP}^{2+} + 1/2\text{Q} + \text{H}^+$$

dx.doi.org/10.1021/ja506987a | J. Am. Chem. Soc. 2014, 136, 13514–13517

In summary, we describe here a facile protocol for stabilizing Ru(II) polypyridyl-derivatized phosphonate and carboxylate complexes on oxide surfaces in water over an extended pH range. It is based on a dip-coating procedure that results in conformal PMMA overlayers of controlled thicknesses on nanoparticle, mesoporous films of TiO_2 or nanoITO. Electron transfer reactivity is retained on the stabilized surfaces with $E_{1/2}$ and peak currents for the Ru(III/II) couples relatively unaffected by overlayer thicknesses of up to 2.1 nm with potential shifts in $E_{1/2}$ for surface-bound Ru(III/II) couples of less than 0.02 V. The PMMA overlayer procedure results in stabilization of surface binding with thermal and photochemical stabilities of up to 100-fold achieved under basic conditions.

Excitation of the surface-bound, stabilized, Ru(II) polypyridyl dye $\mathbf{RuP^{2+}}$ on TiO_2 is followed by efficient MLCT excited state injection, TiO_2-$\mathbf{RuP^{2+}}$*(PMMA) → $TiO_2(e^-)$-$\mathbf{RuP^{3+}}$(PMMA). Back electron transfer, $TiO_2(e^-)$-$\mathbf{RuP^{3+}}$(PMMA) → TiO_2-$\mathbf{RuP^{2+}}$(PMMA), is pH independent pointing to control of the effective surface pH by the PMMA overlayer dictated by the pH at the surface in the surface loading solution.

The results described here point to PMMA dip-coating as an appealingly simple and surprisingly effective strategy for preparing surface-stabilized chromophore or chromophore−catalyst assembly structures on mesoporous nanostructured metal-oxides in both acidic and basic aqueous solutions for long-term stability in DSPEC and potentially electrocatalytic applications. Experiments currently in progress point to the PMMA stabilization procedure as being a general approach providing surface stabilization for organic dyes, water oxidation catalysts, and chromophore−catalyst assemblies.

■ ASSOCIATED CONTENT

Ⓢ Supporting Information

Experimental details, SEM/TEM images, and photostability in various pH conditions of PMMA-coated TiO_2 or nanoITO film. This material is available free of charge via the Internet at http://pubs.acs.org.

■ AUTHOR INFORMATION

Corresponding Author

tjmeyer@unc.edu

Notes

The authors declare no competing financial interest.

■ ACKNOWLEDGMENTS

This research was primarily supported by the UNC EFRC Center for Solar Fuels, an Energy Frontier Research Center funded by the U.S. Department of Energy, Office of Science, Office of Basic Energy Sciences under Award Number DE-SC0001011, supporting M.K.B., L.A., B.H.F., and B.S. In addition, K.-R.W. acknowledges a fellowship from the Basic Science Research Program through the National Research Foundation of Korea (NRF) funded by the Ministry of Education (2013R1A6A3A03058617) for financial support. A.M.L. acknowledges support from the United States Government under FA9550-11-C-0028 and awarded by the Department of Defense, Air Force Office of Scientific Research, National Defense Science and Engineering Graduate (NDSEG) Fellowship, 32 CFR 168a. We also thank Dr. Amar Kumbhar (CHANL) for assistance with FIB-SEM and TEM measurements.

■ REFERENCES

(1) Barber, J.; Andersson, B. *Nature* **1994**, *370*, 31.
(2) Alstrum-Acevedo, J. H.; Brennaman, M. K.; Meyer, T. J. *Inorg. Chem.* **2005**, *44*, 6802.
(3) Barber, J. *Chem. Soc. Rev.* **2009**, *38*, 185.
(4) Walter, M. G.; Warren, E. L.; McKone, J. R.; Boettcher, S. W.; Mi, Q.; Santori, E. A.; Lewis, N. S. *Chem. Rev.* **2010**, *110*, 6446.
(5) Cook, T. R.; Dogutan, D. K.; Reece, S. Y.; Surendranath, Y.; Teets, T. S.; Nocera, D. G. *Chem. Rev.* **2010**, *110*, 6474.
(6) Liu, C.; Dasgupta, N. P.; Yang, P. *Chem. Mater.* **2014**, *26*, 415.
(7) McKone, J. R.; Lewis, N. S.; Gray, H. B. *Chem. Mater.* **2014**, *26*, 407.
(8) Gratzel, M. *Nature* **2001**, *414*, 338.
(9) Lewis, N. S.; Nocera, D. G. *Proc. Natl. Acad. Sci. U.S.A.* **2006**, *103*, 15729.
(10) Concepcion, J. J.; House, R. L.; Papanikolas, J. M.; Meyer, T. J. *Proc. Natl. Acad. Sci. U.S.A.* **2012**, *109*, 15560.
(11) Moore, G. F.; Blakemore, J. D.; Milot, R. L.; Hull, J. F.; Song, H.-E.; Cai, L.; Schmuttenmaer, C. A.; Crabtree, R. H.; Brudvig, G. W. *Energy Environ. Sci.* **2011**, *4*, 2389.
(12) Swierk, J. R.; Mallouk, T. E. *Chem. Soc. Rev.* **2013**, *42*, 2357.
(13) Young, K. J.; Martini, L. A.; Milot, R. L.; Snoeberger, R. C.; Batista, V. S.; Schmuttenmaer, C. A.; Crabtree, R. H.; Brudvig, G. W. *Coord. Chem. Rev.* **2012**, *256*, 2503.
(14) Alibabaei, L.; Brennaman, M. K.; Norris, M. R.; Kalanyan, B.; Song, W.; Losego, M. D.; Concepcion, J. J.; Binstead, R. A.; Parsons, G. N.; Meyer, T. J. *Proc. Natl. Acad. Sci. U.S.A.* **2013**, *110*, 20008.
(15) Alibabaei, L.; Luo, H.; House, R.; Hoertz, P.; Lopez, R.; Meyer, T. J. *J. Mater. Chem. A* **2013**, *1*, 4133.
(16) Hanson, K.; Losego, M. D.; Kalanyan, B.; Parsons, G. N.; Meyer, T. J. *Nano Lett.* **2013**, *13*, 4802.
(17) Hanson, K.; Brennaman, M. K.; Luo, H.; Glasson, C. R. K.; Concepcion, J. J.; Song, W.; Meyer, T. J. *ACS Appl. Mater. Interfaces* **2012**, *4*, 1462.
(18) Tanaka, H.; Takeichi, A.; Higuchi, K.; Motohiro, T.; Takata, M.; Hirota, N.; Nakajima, J.; Toyoda, T. *Sol. Energy Mater. Sol. Cells* **2009**, *93*, 1143.
(19) Wang, D.; Wang, G.; Zhao, J.; Chen, B. *Chin. Sci. Bull.* **2007**, *52*, 2012.
(20) Hanson, K.; Losego, M. D.; Kalanyan, B.; Ashford, D. L.; Parsons, G. N.; Meyer, T. J. *Chem. Mater.* **2012**, *25*, 3.
(21) Ashford, D. L.; Lapides, A. M.; Vannucci, A. K.; Hanson, K.; Torelli, D. A.; Harrison, D. P.; Templeton, J. L.; Meyer, T. J. *J. Am. Chem. Soc.* **2014**, *136*, 6578.
(22) Lapides, A. M.; Ashford, D. L.; Hanson, K.; Torelli, D. A.; Templeton, J. L.; Meyer, T. J. *J. Am. Chem. Soc.* **2013**, *135*, 15450.
(23) Moss, J. A.; Yang, J. C.; Stipkala, J. M.; Wen, X.; Bignozzi, C. A.; Meyer, G. J.; Meyer, T. J. *Inorg. Chem.* **2004**, *43*, 1784.
(24) Hager, G. D.; Crosby, G. A. *J. Am. Chem. Soc.* **1975**, *97*, 7031.
(25) Hecker, C. R.; Fanwick, P. E.; McMillan, D. R. *Inorg. Chem.* **1991**, *30*, 659.
(26) Thompson, D. W.; Fleming, C. N.; Myron, B. D.; Meyer, T. J. *J. Phys. Chem. B* **2007**, *111*, 6930.
(27) Brennaman, M. K.; Patrocinio, A. O. T.; Song, W.; Jurss, J. W.; Concepcion, J. J.; Hoertz, P. G.; Traub, M. C.; Murakami Iha, N. Y.; Meyer, T. J. *ChemSusChem* **2011**, *4*, 216.
(28) Hanson, K.; Brennaman, M. K.; Ito, A.; Luo, H.; Song, W.; Parker, K. A.; Ghosh, R.; Norris, M. R.; Glasson, C. R. K.; Concepcion, J. J.; Lopez, R.; Meyer, T. J. *J. Phys. Chem. C* **2012**, *116*, 14837.
(29) Farnum, B. H.; Morseth, Z. A.; Lapides, A. M.; Rieth, A. J.; Hoertz, P. G.; Brennaman, M. K.; Papanikolas, J. M.; Meyer, T. J. *J. Am. Chem. Soc.* **2014**, *136*, 2208.
(30) Knauf, R. R.; Brennaman, M. K.; Alibabaei, L.; Norris, M. R.; Dempsey, J. L. *J. Phys. Chem. C* **2013**, *117*, 25259.
(31) Chen, P.; Meyer, T. J. *Chem. Rev.* **1998**, *98*, 1439.